Presented at 1976, IEEE
EMC International Symposium
Washington, D.C.
July 13, 1976

Transfer Impedance and Transfer Admittance Measurements on Gasketed Panel Assembles and Honeycomb Air-Vent Assemblies

P. J. Madle, Senior Member, IEEE

Summary — Electromagnetic energy can penetrate incompletely shielded enclosures through the action of three different coupling mechanisms. Two of these mechanisms, diffusion through the thickness of the shield and magnetic field coupling through imperfections in the shield, can be combined and represented as a Transfer Impedance which relates the magnetic field at the outer surface of the enclosure to the resulting electric field induced along the inner surface.

The third of these coupling mechanisms, electric field coupling through imperfections in the shield, can be represented as a Transfer Admittance which relates the electric field normal to the outer surface of the enclosure to the resulting magnetic field induced at the inner surface.

The electric and magnetic fields at the outer surface of the enclosure could be directly resultant from some incident electromagnetic field or could be themselves induced by electromagnetic energy flowing along the surface of the shield from some remote source.

Two test fixtures are described, one for the measurement of Transfer Impedance and one for Transfer Admittance. A limited amount of test data obtained on several types of gasket materials, used in several assembly configurations is shown. This data demonstrates the effects of different conductive surface coatings, pressures, and geometries. Some test data showing the use of the same test fixtures for honeycomb air-vent materials is included. The specific test fixtures are sized to allow measurements from D.C. to 0.7 GHz and are designed to allow easv interchange of test samples.

I. Introduction

The shielding performance of a gasketted joint in a conductive sheet can be represented by a Transfer Impedance and a Transfer Admittance. This paper reviews the mechanisms controlling the shielding performance and suggests test configurations so that measured values of the parameters can be used in analyses of systems containing such gasketted joints.

A shielded enclosure is intended to isolate electrical circuits from an external electromagnetic environment. Many authors including Schelkunoff[1], Marcuvitz[2] and Bridges[3] have analyzed the mechanisms by which such electromagnetic energy can penetrate the shield and induce unwanted signals on the conductors. The mechanisms of interest are, diffusion through the thickness of the shield material, and both electric and magnetic field coupling through apertures or imperfections in the shield material. Analysis of types suggested by these authors is of great value to a hardware designer since optimum materials and dimensions can be chosen for the basic shield arrangement desired, however, many designs involve gasketted panels, honeycomb air-vents, mechanical joints or inhomogenities which are very difficult to analyze. For such reasons most design efforts commence with analyses of those parts of the structure for which mathematical treatments exist or for which parameter values can be determined and then progress to detailed design decisions requiring engineering judgment. Finally, verification testing is performed to ensure that the shielding level desired has been achieved.

II. Transfer Impedance

(a) Theory

It has been shown[1,2,3] that the diffusion and magnetic field coupling processes can be combined into an expression for the transfer impedance,

$$Z_{TR} = \frac{V}{I_o} = R_o \frac{\gamma d}{\sinh \gamma d} + j\omega M_{12} \qquad (1)$$

where I_o is the total current flowing in the shield, V is the open circuit voltage generated by this current along the transmission line formed by the shield and the conductors enclosed by the shield, R_o is the dc resistance of the shield, d is the thickness of the shield and M_{12} is the mutual inductance of the shield between the internal and external surfaces. γ is given by $\gamma = (1 + j)/\delta$ where δ is the skin depth in the shield material $\left[\delta = (\pi f \mu \sigma)^{-1/2}\right]$.

A generalization to the form $Z_{TR} = R_J(\omega) + j\omega M_J$ extends the concept of transfer impedance to that of a peripheral joint or other inhomogenity in the shield having a frequency dependent resistance $R_J(\omega)$ and a mutual inductance M_J. Such peripheral joints often occur at interfaces between panels, gaskets and air-vents and are characterized by "contact" resistances, which can be readily measured. However, these contact resistances are usually nonuniformly distributed around the periphery giving rise to mutual inductances M_J which are difficult to measure. Thus the transfer impedance of a shield assembly is independent of how the assembly is incorporated into some overall shielding system. Transfer impedances can be measured in a test fixture and the values incorporated into analyses of the shielding performance of systems.

(b) Test Method

The "Shield Configuration" portion of Figure 1 shows a Panel covering an aperture in a Shield. The exterior surfaces of the Panel and Shield carry a current I_o, induced by external E- or B-fields. Electromagnetic leakage through the gasketted joint, due to resistance or inductance of the joint or to diffusion through the gasket material results in internal E-fields. These fields can induce a current in an internal conductor.

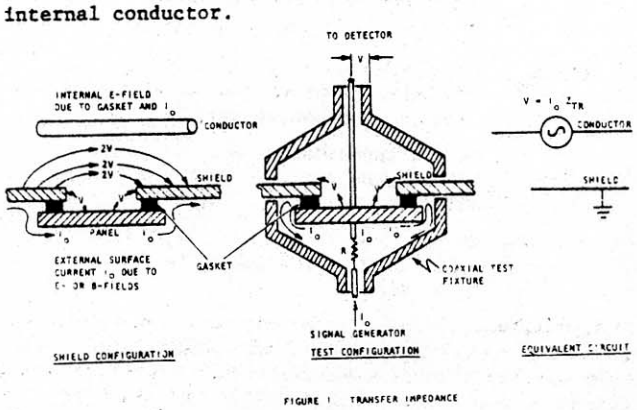

FIGURE 1 TRANSFER IMPEDANCE

The "Test Configuration" portion of Figure 1 shows the same Panel, Gasket and Shield arrangement placed in a test fixture. A signal generator drives curr

I_o onto the external surface of the panel from where it must flow across the gasketted joint to the shield before returning to the signal generator. A voltage V is induced between the interior surfaces of the panel and shield and is measured by a detector. The coaxial test fixtures for the drive-current circuit and the voltage-measuring circuit can support TEM modes up to a frequency at which their periphery is approximately one wavelength. Above this frequency higher order modes can exist the result of which would be that the current I_o and the Voltage V_o could vary in phase and magnitude from point to point around the periphery of the gasket. The resulting complex leakage fields would not result in a meaningful voltage at the detector. These limitations concerning TEM modes are stated in the appendix to MIL-C-39012B[4]:

"The equivalent leakage generator, in general, can have field components in the radial, axial, and circumferential directions. Furthermore, these components are not necessarily circularly symmetric. Locally, TE, TM, and TEM modes can all exist, and in fact, for complete leakage measurements, the detector should couple to all but the measurement is more complex in this case. The excitation of the outer coaxial line, however, is believed to be principally TEM, since the currents in the internal line are predominantly axial and symmetric. It is, however, possible to have a symmetrical leakage current which can generate the above mentioned modes. It is recommended that all measurements be made below the frequency that the higher order modes can propagate in the outer coaxial line."

III. Transfer Admittance

(a) Theory

Electric field coupling through apertures can be expressed in terms of a transfer admittance, [1,2,3]

$$Y_{TR} = \frac{I}{E_o} = j\,\omega\,C_{12} \qquad (2)$$

where E_o is the external E-field normal to the surface of the shield, I is the induced short-circuit current in the internal conductor and C_{12} is the mutual capacitance between the internal conductor and the external environment.

Marcuvitz[2], has shown that the mutual capacitance C_{12} depends on the geometry and materials of the internal conductors, the apertures in the shield and the exterior configuration such that

$$C_{12} = \frac{p\,C_1\,C_2}{\epsilon_o\,\epsilon_{r_1}\,\epsilon_{r_2}} \qquad (3)$$

where p is the electrical polarisability of the aperture

ϵ_o is the permittivity of free space (8.85×10^{-12} farad per meter)

ϵ_{r_1} and ϵ_{r_2} are the relative permittivities of the dielectrics in the external and internal regions respectively

C_1 is the capacitance per unit area between the shield and the external shield environment

C_2 is the capacitance per unit area between the shield and the inner conductors

Thus, unlike the Transfer Impedance which depends only upon the properties of the shield assembly and not upon interactions between the shield and the system of which it is a part, it is seen that the Transfer Admittance depends upon all of these parameters. The polarisability "p" of the aperture in the shield is however a parameter which is unique to a given assembly, thus "p" can be measured in a test apparatus and the result incorporated into the analysis of a system containing the shield assembly, for which the remaining parameters can be determined.

(b) Test Method

The "Shield Configuration" portion of Figure 2 shows an aperture in a Shield and an external E-field E_o incident normal to the surface. Electric field coupling through the aperture induces internal electric and magnetic fields which can couple to internal conductors.

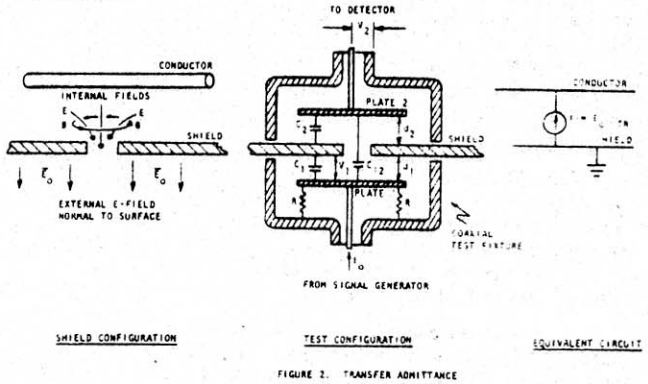

FIGURE 2. TRANSFER ADMITTANCE

The "Test Configuration" portion of Figure 2 shows the same Shield and Aperture. A signal generator drives current I_o through load resistors R causing metal Plate 1 to acquire voltage V_1 with respect to both the coaxial test fixture and the shield under test. Thus an electric field of V_1/d_1 is generated at the surface of the shield. A second plate, Plate 2 in a similar coaxial test fixture is placed over the interior surface of the shield such that mutual capacitance C_{12} between Plates 1 and 2 will couple energy through the aperture. A detector measures this energy as a voltage V_2.

The constraints on the maximum usable frequency are similar to those discussed above in connection with the Transfer Impedance test fixture.

Now for flat plate capacitors with air dielectric the capacitance per unit area is

$$C = \epsilon_o/d$$

where d is the plate separation (meters)

Thus $$C_{12} = p\,\epsilon_o/d_1\,d_2 \qquad (4)$$

and $$Y_{TR} = j\,\omega\,p\,\epsilon_o/d_1\,d_2 \qquad (5)$$

IV. Test Fixture Design

The shielding properties of shield assemblies using gaskets are influenced by the materials and surface finishes of the panels in which they are mounted, by the fasteners used to attain contact pressure and mechanical rigidity and by the relative overlap and spacing of the panel joints. Design engineers require knowledge of all these factors. A standard test panel was chosen, for the purposes of this report, to reduce the number of variables under consideration. This panel is shown in Figure 3. The 20 cm square test panel has a centrally located 10 cm square aperture, covered by a 15 cm square plate fastened by eight #10-32 screws. The screws are arranged so that they can apply pressure to either square or circular gaskets.

If this test method were adopted as an industry standard it would be necessary to use overlaps, fasteners and panel thicknesses appropriate to each type

and dimension of gasket material tested.

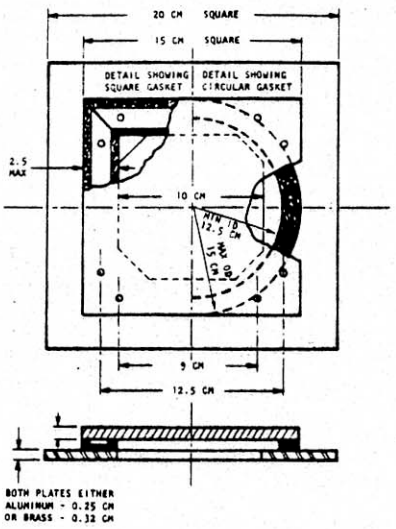

FIGURE 3. TEST PANEL DESIGN

Figure 4 shows the Magnetic-Field Test Fixture equipped with input and output probes mounted in sliding "Iris" glands which allow contact to be made with both sides of the test panel regardless of the thickness of the materials being tested.

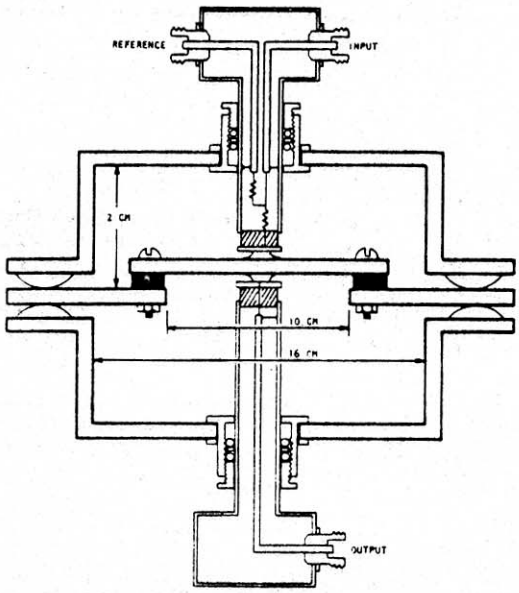

FIGURE 4. MAGNETIC-FIELD TEST FIXTURE

Figure 5 shows the Electric-Field Test Fixture with input and output capacitor plates 9 cm square separated 2.5 cm from the test surfaces.

V. Test Equipment

Figure 6 shows the configuration of Network Analyzer equipment used to cover the frequency range of 100 kHz to 700 MHz.

VI. Test Materials

Table I lists the various materials used in demonstrating the feasibility of the test method. The solid brass and (iridited) aluminum plates were used to determine the noise and leakage limits of the test set. The contact pressure applied to each gasket was not measured but was held reasonably constant at a level just below the onset of distortion of the test panels. Formal testing of gasket materials should, of course, control and measure this pressure.

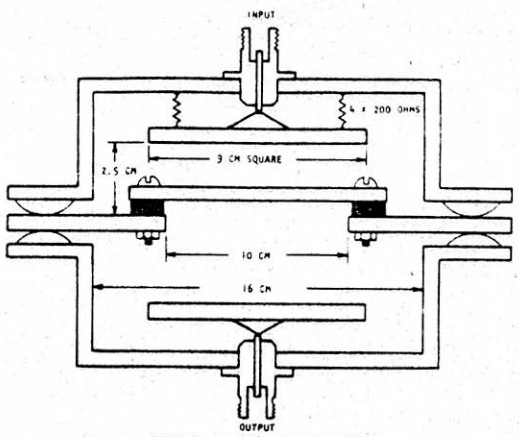

FIGURE 5. ELECTRIC-FIELD TEST FIXTURE

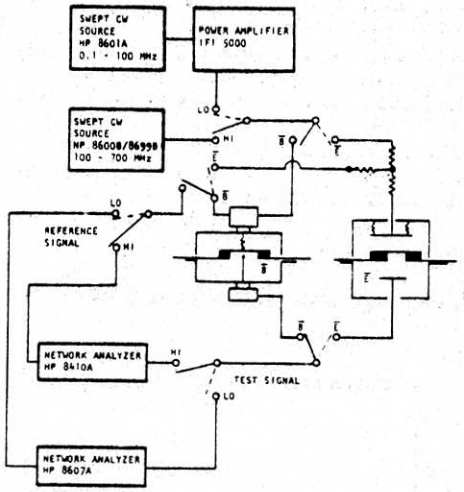

FIGURE 6. TEST EQUIPMENT CONFIGURATION

VII. Test Results — Magnetic Field

Figures 7 through 12 show Transfer Impedance (Z_{TR}), in ohms per centimeter of gasket periphery, versus Frequency for various configurations.

(a) Effects of Materials, Geometry and Fasteners

Figure 7 shows Z_{TR} for the Aluminum and Brass test panels using no gasket, it appears that the Aluminum surfaces have higher resistance than the brass surfaces at low frequencies but that little difference is evident above 10 MHz. Figure 7 also shows the effect of a deliberately "bad" gasket, made of non-conductive neoprene sheet. The transfer impedance thus measured results from the conductivity and self-inductance of the screws used to hold the panels together and from capacitance between the overlapping panels. Practically identical results were obtained using Aluminum panels and Brass panels. The response is well modeled by assuming each screw to have 1 nano-henry of self-inductance and 3 milli-ohms of contact resistance. Four of the eight screws were removed, leaving empty holes, with a resulting 6 dB increase of transfer impedance. Two of the remaining screws were removed, leaving only two screws at diagonally opposite corners. A further 6 dB increase of transfer impedance occurred at low frequencies and a resonant peak appeared at 450 MHz, which is understandable as being due to a slot resonance since the bolts are spaced 30 cm apart, measured along the edge of the panel.

TEST NUMBER		GASKET MATERIAL	WIDTH (cm)	THICKNESS (cm)	SQUARE SHAPE	CIRCULAR SHAPE
WITH BRASS PANEL	WITH IRIDITED ALUMINUM PANEL					
1	-	Solid Brass Plate	-	0.32	-	-
-	2	Solid (Iridited) Aluminum Plate	-	0.25	-	-
100	200	No Gasket Used	-	-	-	-
101	201	Neoprene (Nonconductive) Sheet	0.64	0.24	X	
102	202	Neoprene (Nonconductive) Sheet	0.64	0.48	X	
103	203	Monel Mesh — Compressed	0.64	0.48	X	
104	204	Monel Mesh — Compressed	0.64	0.32	X	
105	205	Monel Mesh over Silicon Foam Core	0.64	0.32		X
106	206	Stainless Steel Spiral	0.36	0.36		X
107	207	Tin-Plated Beryllium Copper Spiral	0.36	0.36		X
108	-	Two Tin-Plated Beryllium Copper Spiral	0.72	0.36		X
109	209	Expanded Monel Sheet	1.0	0.08	X	
110	210	Silver Filled Rubber	2.5	0.16	X	
-	300	0.32 cm Aperture Aluminum Honeycomb	15.0	1.25	X	

TABLE I. TEST MATERIALS

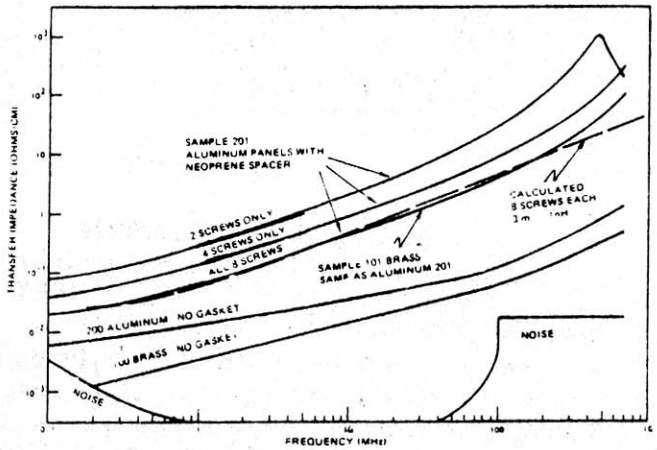

FIGURE 7 MAGNETIC FIELD EFFECTS OF MATERIALS GEOMETRY AND FASTENERS

(b) Iridited Aluminum Panels with Gaskets

Figure 8 shows three types of knitted Monel gasket material and one type of tin-plated material. It is clear that the tin-plated material makes superior ohmic contact and that the Monel materials appear to contribute mainly shunt capacitive coupling across the gap which becomes effective only at high frequencies.

Figure 9 shows the response of other gasket materials including two made of stainless steel but of dissimilar construction and one made of silver conductive filler in a silicon rubber sheet.

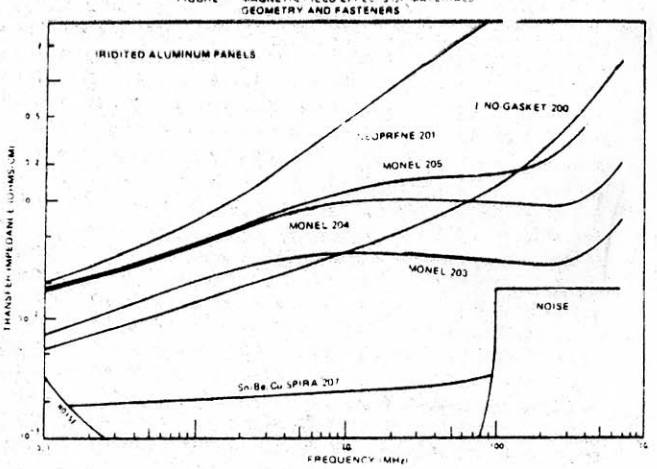

FIGURE 8 MAGNETIC FIELD

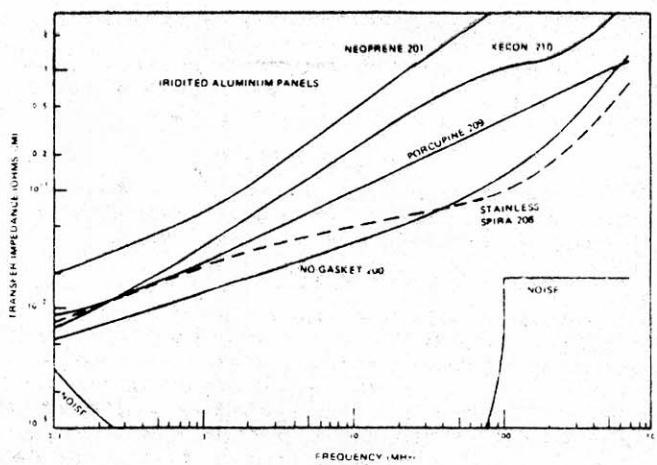

FIGURE 9 MAGNETIC FIELD

(c) Brass Panels with Gaskets

Figures 10 and 11 show the same gaskets used between Brass panels. In general all of the gaskets exhibited a lower transfer impedance when used between Brass panels, with the most marked improvement occurring in the two types of gasket having ohmic surface films, that is the silver and tin-surfaced materials. The other gaskets being made of high-nickel alloys showed less improvement, possibly due to the lower-conductivity of their surface films.

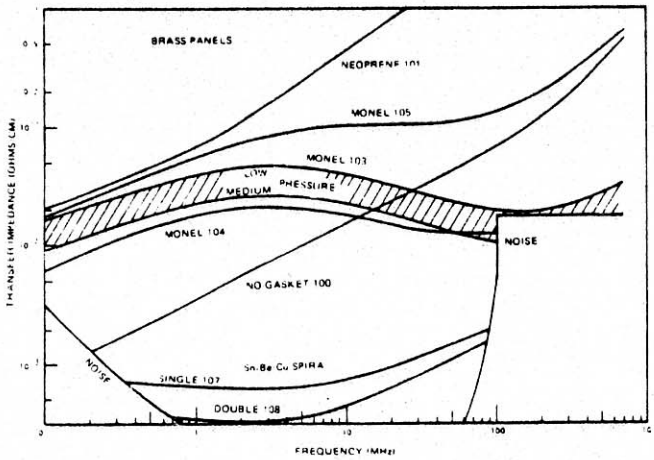

FIGURE 10 MAGNETIC FIELD

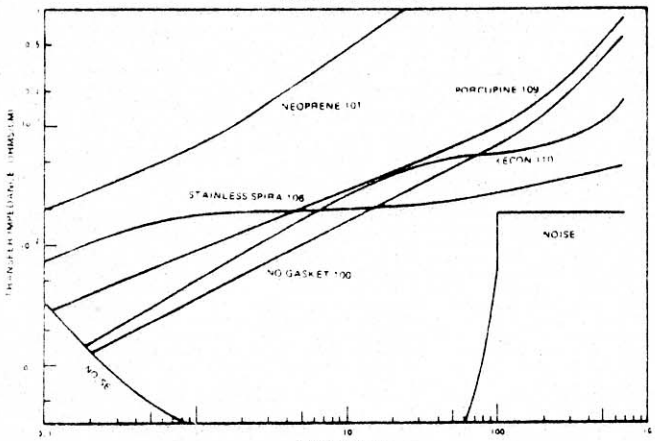

FIGURE 11 MAGNETIC FIELD BRASS PANELS

(d) Honeycomb Air-Vent

One sample of an iridited aluminum honeycomb air-vent complete with aluminum frame and Monel gasket was bolted to an iridited aluminum panel having a 12.5 cm square opening to fit the frame. The transfer function shown on Figure 12 behaves with the anticipated "20 dB per decade" performance expected of the "waveguide beyond cutoff" construction from 100 kHz to 100 MHz but exhibits resonances at higher frequencies.

VIII. Test Results — Electric Field

Figure 13 shows data obtained in the Electric Field Test Fixture. The units plotted are the ratio of Test Signal voltage to Reference Signal voltage using the circuit of Figure 6. This data shows a dependence on frequency to the fourth power, which is not that predicted by equation (5). Review of the Test Fixture resulted in the Equivalent Circuit shown in Figure 14 from which it is seen that energy can not only be coupled by the Mutual Capacitance C_{12}, which forms the Transfer Admittance, but can also be coupled through the direct capacitances C_1 and C_2 and the Transfer Impedance Z_{TR}. Simple analysis of this

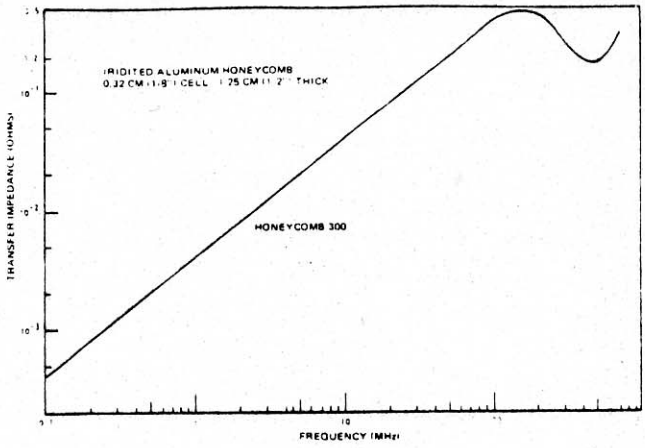

FIGURE 12 MAGNETIC FIELD

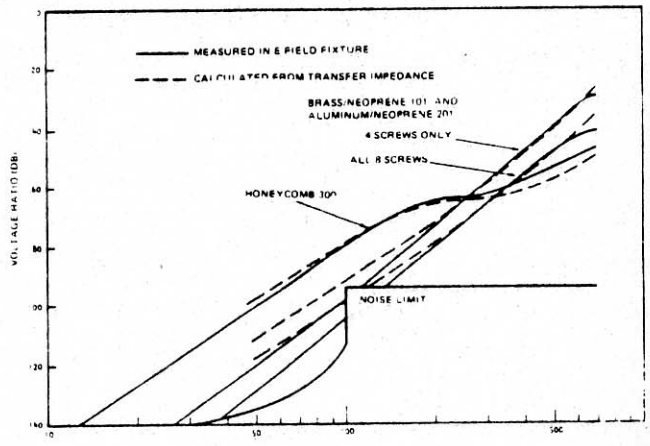

FIGURE 13 ELECTRIC FIELD

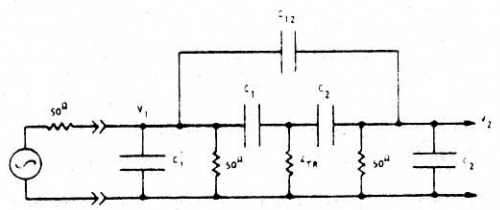

Z_{TR} = TRANSFER IMPEDANCE (OHMS)
C_{12} = MUTUAL CAPACITANCE BEING MEASURED ($Y_{TR} = j\omega C_{12}$)
C_1 & C_2 = DIRECT CAPACITANCE TO TEST SAMPLE
C_1' & C_2' = STRAY CAPACITANCES OF TEST FIXTURE
j = PERI

FIGURE 14. ELECTRIC FIELD - EQUIVALENT CIRCUIT

"second" path, ignoring C_{12}, C_1' and C_2' results in the relation

$$\frac{V_2}{V_1} = 50\ \omega^2\ C_1\ C_2\ Z_{TR} \qquad (6)$$

Figure 13 also shows the calculated values resulting from this relation, using the measured values of the Transfer Impedance Z_{TR}, capacitance C_1 (3×10^{-12} farad for all test samples except for the Honeycomb for which $C_1 = 6 \times 10^{-12}$ farad), and capacitance C_2 (3×10^{-12} farad for all test samples).

It is apparent that the calculated and measured data agree within reasonable experimental accuracy, thus indicating that the Transfer Admittance ($j\omega C_{12}$) contributes negligible coupling compared to that due to the Transfer Impedance.

All other Test Samples were measured, most of them giving low or unreadable signals due to their lower transfer impedance than the examples plotted.

IX. Conclusion

It is concluded that:

1. The Magnetic Field test fixture can be used to measure the Transfer Impedance of a gasketted panel assembly and that this measured data can be used in the analysis of both the Magnetic and Electric Field performance of a system including the gasketted assembly.
2. The Transfer Impedance of an assembly depends upon
   a) The panel materials and surface finish used
   b) The fasteners, spacing, pressure, overlap and geometrical features
   c) The gasket material used
3. The Transfer Admittance of the assemblies tested was not of significance.

X. Acknowledgments

Grateful acknowledgments are made to TRW Inc. for provision of technical assistance, to Mr. A. Toro for construction of the test apparatus and to Kern Manufacturing Inc. for provision of the adjustable "Iris" devices used in this feasibility demonstration.

References

1. S. Schelkunoff, "Electromagnetic Waves," D. Van Nostand Co., Inc., Jan. 1943.
2. N. Marcuvitz, Waveguide Handbook, MIT, Rad. Lab. Ser., vol. 10 (McGraw-Hill, New York, 1951).
3. J. E. Bridges and D. A. Miller, "Standard EMC Cable Parameter Measurements," IEEE Symposium, pages 946 - 951, June 1969.
4. MIL-C-39012B Amendment 1, 18 Oct. 1972, "Military Specification, Connectors, Coaxial, Radio Frequency, General Specifications For."